Coronary Vessel Development Is Dependent on the Type III Transforming Growth Factor β Receptor

Leigh A. Compton, Dru A. Potash, Christopher B. Brown, Joey V. Barnett

Abstract—Transforming growth factor (TGF)β receptor III (TGFβR3), or β-glycan, binds all 3 TGFβ ligands and inhibin with high affinity but lacks the serine/threonine kinase domain found in the type I and type II receptors (TGFβR1, TGFβR2). TGFβR3 facilitates signaling via TGFβR1/TGFβR2 but also has been suggested to play a unique and nonredundant role in TGFβ signaling. Targeted deletion of *Tgfbr3* revealed a requirement for *Tgfbr3* during development of the coronary vessels. Coronary vasculogenesis is significantly impaired in null mice, with few vessels evident and numerous, persistent blood islands found throughout the epicardium. *Tgfbr3*-null mice die at embryonic day 14.5, the time when functional coronary vasculature is required for embryo viability. However, in null mice nascent coronary vessels attach to the aorta, form 2 coronary ostia, and initiate smooth muscle recruitment by embryonic day 14. Analysis of earlier developmental stages revealed defects in the epicardium. At embryonic day 13.5, these defects include an irregular and hypercellular epicardium with abundant subepicardial mesenchyme and a thin compact zone myocardium. *Tgfbr3*-null mice also displayed other defects in coronary development, including dysmorphic and distended vessels along the atrioventricular groove and subepicardial hemorrhage. In null mice, vessels throughout the yolk sac and embryo form and recruit smooth muscle in a pattern indistinguishable from heterozygous or wild-type littermates. These data demonstrate a requirement for *Tgfbr3* during coronary vessel development that is essential for embryonic viability. **(*Circ Res*. 2007;101:000-000.)**

Key Words: coronary vessels ■ transforming growth factor β receptor ■ mice, null

Coronary artery disease is responsible for 54% of all cardiovascular disease in the United States.[1] Coronary vessels have a unique derivation from mesothelial cells that form a transitory structure termed the proepicardium. Proepicardial cells are transferred to the heart, form the epicardium, and give rise to endothelial cells, smooth muscle cells, and cardiac fibroblasts (reviewed elsewhere[2,3]). Endothelial cells derived from the epicardium form a vascular plexus by the process of vasculogenesis. This vascular network attaches to the aorta and recruits epicardially derived mesenchyme to become vascular smooth muscle. The identification of the molecular and cellular processes that regulate coronary vessel development may provide insight into coronary vessel disease and reveal novel therapeutic opportunities.

The transforming growth factor (TGF)β family of growth factors regulates cell growth and differentiation in the cardiovascular system during both development and disease.[4–6] Three ligands, TGFβ1, TGFβ2, and TGFβ3,[7–9] bind 4 cell surface proteins. These include two transmembrane serine/threonine kinase receptors, the type I TGFβ receptor (TGFβR1) and the type II TGFβ receptor (TGFβR2).[10–12] Several type I receptors, termed activin receptor–like kinases (ALKs), have been described. TGFβR2 has a constitutively active cytoplasmic kinase domain and an extracellular domain that binds TGFβ1 and TGFβ3 with high affinity.[13] Ligand binding results in TGFβR2 phosphorylating TGFβR1 (specifically ALK5) and subsequent stimulation of ALK5 kinase activity.[14] ALK5 phosphorylates specific receptor Smads that associate with Smad4 and enter the nucleus to alter gene transcription.[15] A second class of TGFβ binding proteins contains 2 transmembrane proteins, termed the type III TGFβ receptor (TGFβR3), or β-glycan, and endoglin. Both TGFβR3 and endoglin contain a short, highly conserved intracellular domains with no apparent signaling function.[16–18]

The targeted inactivation of several components of the TGFβ signaling pathway result in specific vascular defects.[19,20] The most severe phenotypes are seen after deletion of *Tgfr2* or *Tgfb1*, which results in defects in vasculogenesis and embryonic death.[21,22] Less severe defects characterized by deficits in angiogenesis are noted in mice null for ALK5,[23] ALK1,[24] endoglin,[25] and smad5.[26,27] The role of these molecules in angiogenesis is supported by studies of endothelial cells in culture that reveal TGFβ1 signals via endoglin to regulate the activation of ALK1 and ALK5 to direct endothelial cell proliferation and migration.[28–30] Furthermore, mutations in *ENG* and *ALK1* are responsible for a human disease characterized by defective vascular remodeling, he-

Original received March 27, 2007; revision received July 2, 2007; accepted August 7, 2007.
From the Departments of Pharmacology (L.A.C., D.A.P., J.V.B.) and Pediatrics (C.B.B.), Vanderbilt University Medical Center, Nashville, Tenn.
Correspondence to Joey V. Barnett, PhD, Department of Pharmacology, Vanderbilt University Medical Center, Room 476 RRB, 2220 Pierce Ave, Nashville, TN 37232-6600. E-mail joey.barnett@vanderbilt.edu

Circulation Research **is available at http://circres.ahajournals.org** **DOI: 10.1161/CIRCRESAHA.107.152082**

Percentage of Observed Defects in Embryos

Ventricular Septal Defect	Thin Myocardium	DORV/OA	Ostia	Dysmorphic Vessels
72.7% (16/22)	40% (8/20)	63.6% (14/22)	93.8% (15/16)	88.2% (15/17)

DORV indicates double-outlet right ventricle; OA, overriding aorta.

reditary hemorrhagic telangiectasia.[24,25,31,32] Deletion of the ligand that is uniquely bound with high affinity by TGFβR3, *Tgfb2*, results in a spectrum of severe cardiac defects that include double-outlet right ventricle, ventricular septal defect, and hyperplastic cushions[8,33] but no defects in blood vessel development. A prior report of *Tgfbr3* deletion noted only myocardial thinning and ventricular septal defect with embryonic lethality attributed to liver defects.[34]

Here we report that *Tgfbr3* is required for coronary vessel development. In *Tgfbr3* nulls, the proepicardium is transferred to the heart and the epicardium is formed. Endothelial cells are present, and vasculogenesis is initiated but to a lesser extent than in wild-type or heterozygote embryos. Nascent coronary vessels form properly placed ostia and recruit smooth muscle. However, the reduced coronary vessels are apparently unable to support the needs of the myocardium resulting in death at embryonic day (E)14.5. Vasculature outside of the coronary circulation appears normal.

Materials and Methods

Generation of Null Mice

A targeting vector was made to delete exon 3 that encodes the N terminus, including a portion of the extracellular ligand binding domain. Construction and validation of the targeting vector is described in the online data supplement at http://circres.ahajournals.org (see supplemental Figure I).

Histology, Whole-Mount Immunohistochemistry, and β-Galactosidase Staining

Detailed methodology is described in the online data supplement.

Results

Deletion of Tgfbr3 Results in Embryonic Lethality

Exon 3 was targeted as depicted in the online data supplement (supplemental Figure I). Matings between heterozygous nulls failed to produce any live homozygous null embryos after E14.5, suggesting that the null allele is embryonic lethal (supplemental Table I). Embryos harvested before E14.0 appeared grossly normal. Examination of null embryos revealed defects in outflow tract (OFT) morphogenesis (Table). At E14.5, wild-type and heterozygous null mice have a septated OFT and a discrete aorta and pulmonary trunk with properly formed valves (Figure 1). Defects in null embryos ranged from overriding aorta to double-outlet right ventricle (Figure 1), suggesting defects in OFT wedging required for proper alignment over the left and right ventricles. Consistent with a prior report,[34] we noted a high incidence of ventricular septal defect and thin compact zone myocardium (Table). Although significant, these defects are unlikely to be responsible for embryonic death at E14.5.

Tgfbr3-Null Mice Display Defects in Coronary Vasculogenesis

Because embryonic death coincides temporally with the known dependency of embryo viability on the formation of the coronary circulation, we examined null embryos for the presence of coronary vessels. Whole-heart immunostaining for the vascular endothelial cell marker platelet endothelial cell adhesion molecule (PECAM) (also known as CD31) at E14.0 revealed dramatically decreased immunoreactivity in nulls (Figure 2A and 2B). The developing vascular plexus was much less pronounced in null embryos, and fewer vessels formed on both the ventral and dorsal surfaces of the heart (Figure 2). The large vessels present in wild-type and heterozygous hearts were absent in nulls. Null hearts often had PECAM-positive structures reminiscent of blood islands. Sectioning confirmed fewer PECAM-positive cells in the subepicardial space and myocardium of null mice (data not

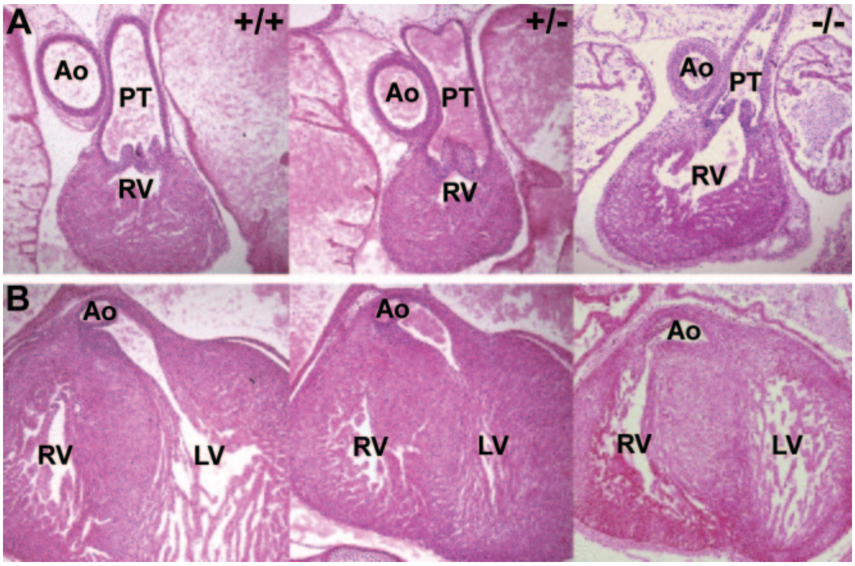

Figure 1. Double outlet right ventricle in *Tgfbr3*-null embryos. A and B, Sections of the OFT region of embryos harvested at E15.5. Wild-type and heterozygous null embryos were viable. Nulls were not viable, with development arrested at E14.5. The pulmonary artery arises from the right ventricle in wild-type, heterozygous, and null embryos (A). The aorta arises from the left ventricle in wild-type and heterozygous embryos and from the right ventricle in nulls (B). Sections stained with hematoxylin and eosin. Photomicrographs at ×200 magnification. Ao indicates aorta; PT, pulmonary trunk; RV, right ventricle; LV, left ventricle.

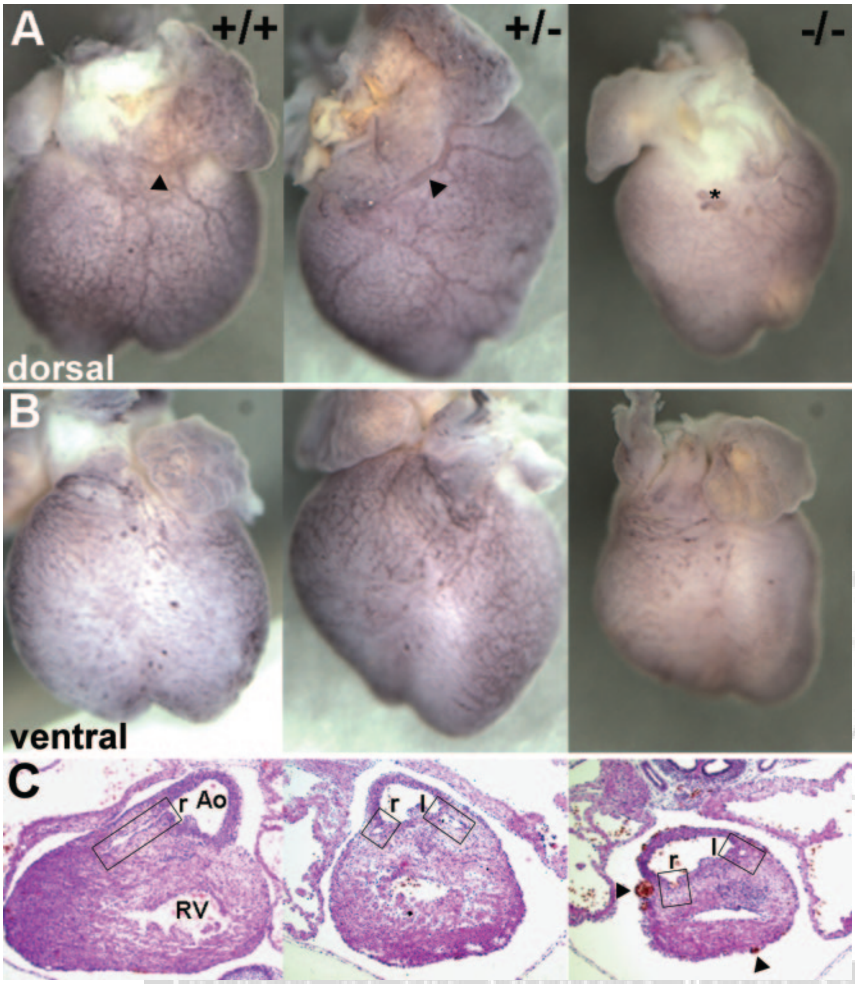

Figure 2. Coronary vessel and ostia formation at E14.0. A and B, Whole hearts immunostained for PECAM. Wild-type and heterozygous null hearts have a dense, PECAM-positive vascular plexus on the dorsal surface of the heart and multiple large vessels have formed by vascular remodeling (arrowheads) (A). Formation of the primitive vascular plexus has spread from the dorsal to ventral surface (B). Null hearts have a poorly formed vascular plexus on the dorsal and ventral surfaces and a lack of large remodeled vessels on the dorsal surface. Irregularly shaped PECAM-positive structures were noted (asterisk) (A). C, Photomicrographs of hematoxylin and eosin–stained sections of the heart at the level of the aorta and right ventricle. Wild-type and heterozygous mice form right and left coronary ostia (open boxes). Homozygous null mice form ostia indistinguishable from wild-type and heterozygous embryos (open boxes). Multiple blood islands are present in the null epicardium (arrowheads).

shown). No gross differences in heart size were noted among genotypes.

We next asked whether the few coronary vessels found in nulls were patent with the systemic circulation. Coronary arteries formed by vasculogenesis attach to the systemic circulation around E14.0 via 2 coronary ostia that reside superior to the right and left aortic valve leaflets. Embryos were sectioned and examined for the presence of patent ostia (Figure 2C). Null embryos were scored relative to wild-type and heterozygous null littermates. In nulls, right and left ostia were seen in 15 of 16 embryos examined. In contrast to wild-type or heterozygous embryos, nulls exhibited persistent blood islands in the region of the coronary ostia. These data suggest that although vasculogenesis and vessel formation is impaired in null embryos, the resulting vessels properly attach to the systemic circulation.

Tgfbr3-Null Mice Have Abnormal Epicardium and Dysmorphic Coronary Vessels

The epicardium is derived from the proepicardium and contains coronary vessel precursor cells. At E13.5, the epicardium forms a tightly apposed monolayer on the surface on the atria and ventricles. In the region of the atrioventricular groove, the epicardium is separated from the myocardium by a layer of epicardial-derived mesenchyme (Figure 3A). The epicardium of heterozygous embryos was indistinguishable from wild-type embryos. However, we observed multiple defects in the epicardium of nulls. At E13.5, the separation between the epicardium and myocardium is expanded and contains numerous mesenchymal cells (Figure 3A). This thick, hypercellular layer expands across the surface of the ventricles and along the atria (Figure 4A and 4B). In contrast to the few, small blood islands still present in wild-type or heterozygous embryos, blood islands in the subepicardial space of nulls are large and abundant (Figure 4B [asterisk] and 4C [arrowheads]). Null embryos often had red blood cells in the ventricular subepicardium (Figure 3C).

At E13.5, blood vessels can be seen forming in the subepicardial mesenchyme in the atrioventricular groove in wild-type and heterozygous embryos. The lumens of these vessels are round and enclosed by endothelial cells (Figure 3B). In contrast, vessels formed in nulls are irregularly shaped (Figure 3B and the Table). These defects in epicardium and blood vessel development are accompanied by a thin compact zone myocardium (Figure 3C).

Tgfbr3-Null Mice Initiate Recruitment of Smooth Muscle to Extracardiac and Coronary Vessels

TGFβ has multiple roles during blood vessel formation, including vascular smooth muscle cell recruitment.[35] To

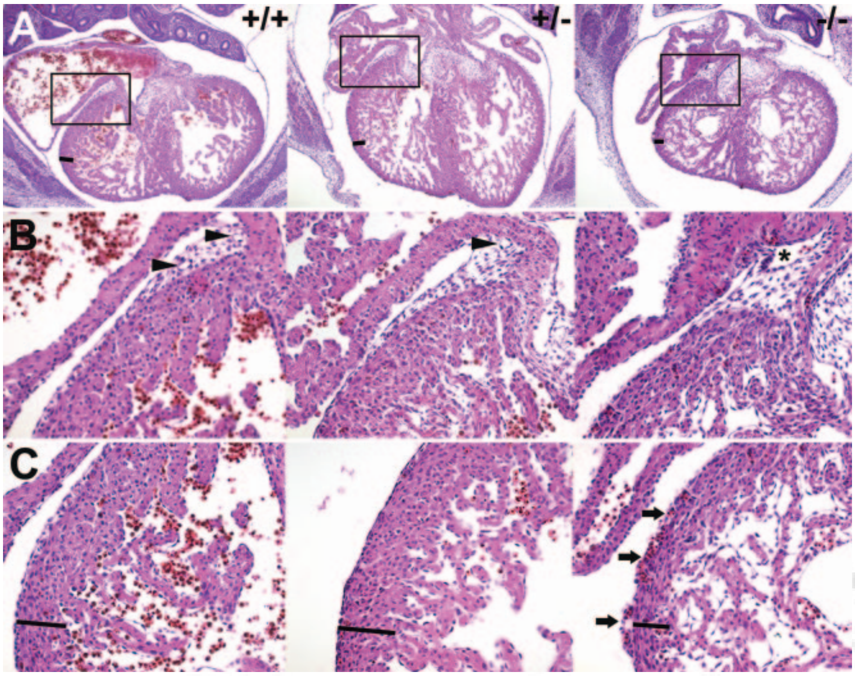

Figure 3. Null mice display distended coronary vessels and subepicardial hemorrhage. A and B, Photomicrographs of sections of subepicardial vessels in the atrioventricular groove and epicardium along the ventricular myocardium at E13.5. Wild-type and heterozygous embryos display numerous vessels in the subepicardial space (arrowheads), and the epicardium is closely apposed to the ventricular myocardium (A and B). Null embryos display distended vessels in the subepicardium (asterisks) (B), and blood cells are evident in the epicardium along the ventricles (arrows) (C). Null mice have a relatively thin ventricular compact zone myocardium (bars) (C). All sections were stained with hematoxylin and eosin. Photomicrographs at ×400 magnification.

examine the association of vascular smooth muscle with blood vessels in nulls, heterozygous null mice were crossed to mice that express *lacZ* under the control of the smooth muscle 22α promoter (SM22α*lacZ*).[36] Whole-mount staining of E14.0 embryos produced by matings between *Tgfbr3*$^{+/-}$;SM22α*lacZ* mice revealed no gross difference in the pattern of *lacZ* expression in nulls when compared with wild-type and heterozygous nulls (Figure 5A). This is despite evidence of hemodynamic failure in nulls. Examination of the extraembryonic vasculature revealed no apparent difference in vascular patterning or smooth muscle recruitment in the yolk sac (Figure 5B). These data demonstrate that defects in vasculogenesis in nulls are limited to the coronary vasculature.

After right and left coronary arteries attach to the systemic circulation at the aorta, smooth muscle recruitment commences at the coronary ostia and progresses distally. As noted in Figure 2, null mice form 2 coronary ostia, similar to wild-type mice, but die shortly after the start of smooth muscle recruitment. At E14.0, SM22α*lacZ*-positive cells are not associated with large, subepicardial vessels in wild-type, heterozygous, or null hearts (Figure 6A and 6B). Transgene expression in the OFT is indistinguishable among genotypes. One day later in development at E15.0, *lacZ*-positive cells are associated with large subepicardial blood vessels on both the dorsal and ventral surfaces of the heart in wild-type embryos (supplemental Figure IIC); no nulls survive to E15.0. At

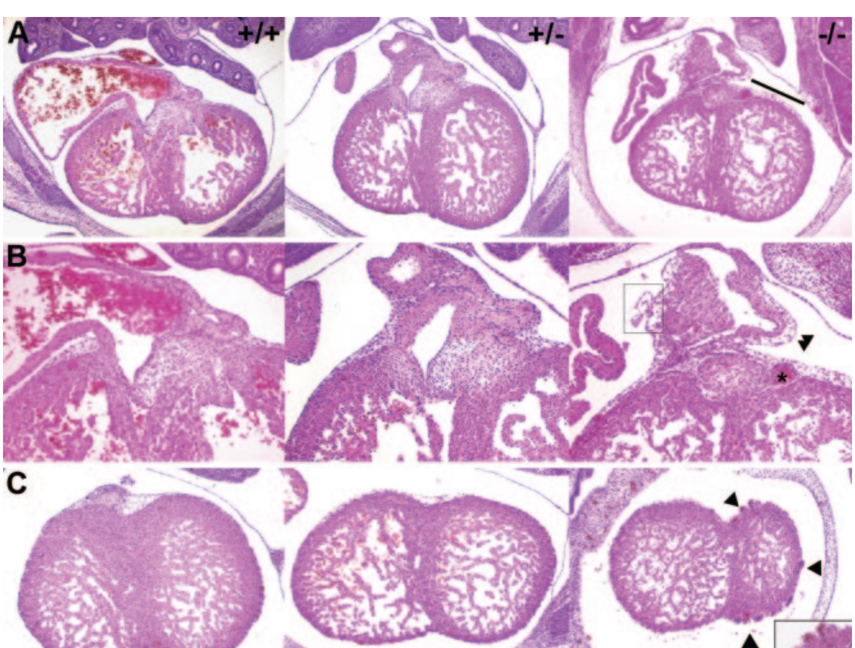

Figure 4. Thickened epicardium and blood islands in null embryos. A through C, Photomicrographs of sections of E13.5 hearts at the level of the atrial root (A and B) or superior margin of the liver (C). In wild-type and heterozygous mice, the epicardium is tightly apposed to the myocardium along the ventricles. In nulls, subepicardial mesenchyme is present along the surface of the ventricles (bar) (A) and atrial root (large double arrowheads and box) (B). Wild-type and heterozygous embryos lack blood islands and pericardial hemorrhage. In null embryos, large blood islands are present in the subepicardium (asterisks in B; arrowheads and inset in C). Pericardial hemorrhage is present. All sections were stained with hematoxylin and eosin. Magnification: ×100 (A and C); ×200 (B); ×400 (inset in C).

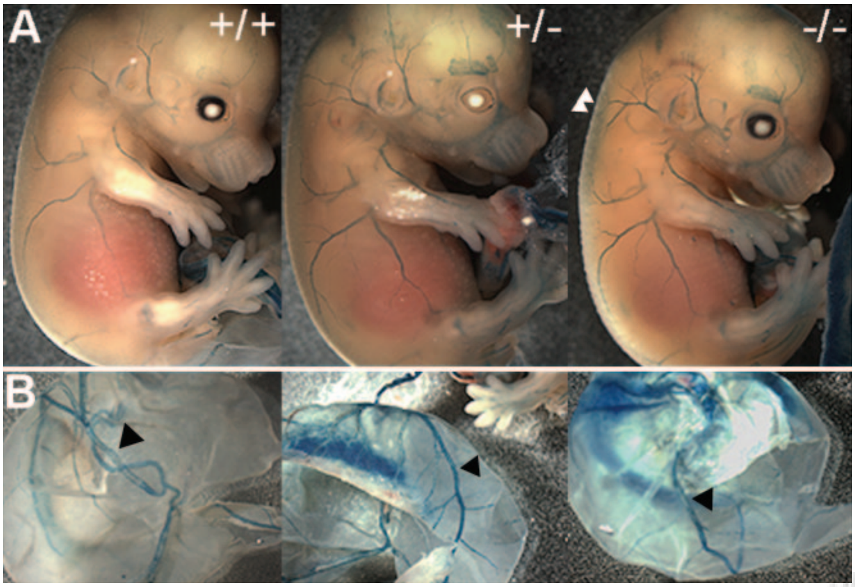

Figure 5. Vascular development and smooth muscle recruitment are grossly normal. A and B, Photomicrographs of E14.0 β-galactosidase–stained embryos carrying the SM22α-*lacZ* transgene. A, Wild-type and heterozygote embryos show similar vascular patterning and smooth muscle recruitment. In nulls, vessel patterning and smooth muscle recruitment is indistinguishable from controls. Edema is evident in nulls (double arrowhead). B, Similar vascular patterning and smooth muscle recruitment is seen in the yolk sac (arrows) in all genotypes.

E14.5, *lacZ*-positive cells surround both right and left coronary ostia in wild-type, heterozygous, and null embryos (Figure 6C). In addition, Sm22α*lacZ* expression is also noted in a subpopulation of cells in the epicardial layer and subepicardial mesenchyme. Positive cells in the subepicardial mesenchyme are not associated with nascent vessels (supplemental Figure IIA). Null embryos have a similar pattern of *lacZ* expression, with abundant expression found in cells associated with blood-filled, dysmorphic vessels (supplemental Figure IIA). In all genotypes, at E14.0 blood islands are found at the apex of the heart associated with *lacZ*-positive cells (supplemental Figure IIB). Smooth muscle recruitment appears to occur normally in all tissues examined, including nascent coronary vessels. However, because null mice die while smooth muscle recruitment is occurring, we cannot rule out a role for *Tgfbr3* during later stages of coronary vascular smooth muscle recruitment.

Discussion

Disruption of *Tgfbr3* revealed a requirement for coronary vessel development and embryonic viability. Null embryos die at E14.5 with defects in coronary vessel development, whereas vasculature outside of the coronary circulation appears normal. Although greatly reduced in size, nascent coronary vessels attach to the aorta and initiate smooth muscle recruitment. Coronary vessel defects are coincident with epicardial abnormalities that include increased space between the epicardium and myocardium, abundant subepi-

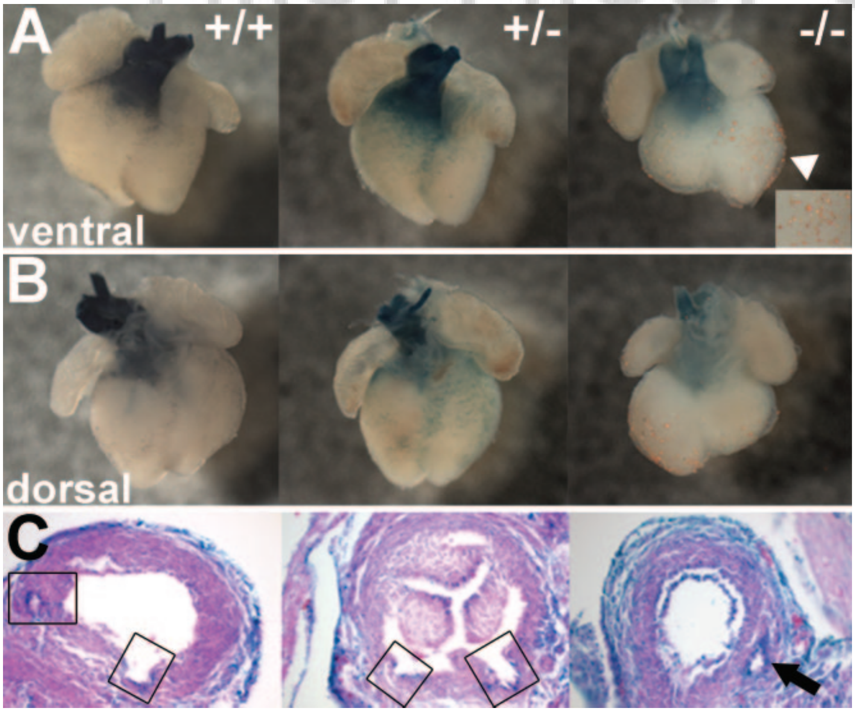

Figure 6. Smooth muscle recruitment to the coronary ostia occurs in null embryos. Photomicrographs of E14.0 β-galactosidase–stained hearts with the SM22α*lacZ* transgene. A and B, The pattern of *lacZ* expression is indistinguishable in all genotypes with prominent expression in the OFT (A, ventral; B, dorsal). In nulls, blood islands and hemorrhage are evident in the epicardium (inset in B), which is widely separated from the myocardium (arrowheads) (B). C, Sections at the level of the aortic root demonstrating the presence and proper placement of coronary ostia (boxes). *lacZ*-positive cells are found in association with the ostia in all genotypes. *lacZ*-positive cells in association with ostia in nulls are denoted by arrow.

cardial mesenchyme, and persistent blood islands. In addition to coronary vessel anomalies, null embryos have OFT abnormalities and myocardial thinning. Presumably, the greatly reduced coronary vasculature in null embryos is not sufficient to adequately perfuse the heart resulting in embryonic death.

Despite the abundance of data implicating TGFβ signaling in vasculogenesis and angiogenesis, these processes appear to occur normally outside of the coronary vessels in nulls. The localization of defects to the coronary vessels may be explained by the unique derivation of these vessels (reviewed elsewhere[2,3]). The proepicardium, adjacent to the liver rudiment, is transferred to the heart and gives rise to the epicardium as well as coronary endothelial cells, smooth muscle cells, and cardiac fibroblasts.[37,38] Endothelial cells delivered to the heart form a vascular plexus, attach to the aorta, and recruit epicardially derived mesenchyme to form vascular smooth muscle. Null mice show defects at multiple stages of coronary vessel formation. In nulls, proepicardial cells are delivered to the heart, form an epicardium and undergo epicardial mesenchymal transformation. However, the epicardium is hypercellular, and the subepicardial space is widened with abundant subepicardial mesenchyme. In contrast, the myocardium is thin, consistent with reduced proliferation in the compact zone myocardium of null embryos.[34] Because *Tgfbr3* is expressed in both myocardium[34] and epicardium (unpublished), and bidirectional signaling between the epicardium and myocardium is required for the proper formation of each,[39–42] the defects described in these tissues may result from a requirement for *Tgfbr3* in epicardium, myocardium, or both.

Although targeted gene deletion in mice has uncovered roles for several molecules in coronary vessel development, none has a phenotype similar to *Tgfbr3* nulls. Deletion of vascular cell adhesion molecule-1[40] or the counter receptor α4 integrin[43,44] results in the loss of the epicardium. Recently, WT-1 has been shown to regulate the expression of α4 integrin,[45] which may explain phenotypic similarities after the loss of WT-1[46] or α4 integrin. Similarly, impairment of GATA4 and FOG2 function disrupts epicardial and myocardial interactions that support epicardial mesenchymal transformation.[42,47] A subtle epicardial phenotype is seen in Cx43-null embryos, in which epicardial cells are rounded in contrast to the flattened shape seen in wild-type embryos.[48] Thymosin β4 is a G actin monomer–binding protein recently identified as a factor from the myocardium that is essential for coronary vessel development and promotes migration and differentiation of adult epicardial cells.[49] Dysregulation of myocardial angiopoietin-1 expression results in 90% embryonic lethality attributable to failed coronary vessel development coincident with an absence of epicardium.[50] Double knockout of *Fgfr1* and *Fgfr2* from the myocardium results in fewer coronary vessels, a morphologically normal epicardium, and impaired formation of subepicardial mesenchyme.[51] Our findings in *Tgfbr3* nulls that include a thickened epicardium with an apparent increase in subepicardial mesenchyme are dissimilar from these described phenotypes, suggesting that the role of TGFβR3 in the regulation of epicardial cell behavior may be distinct from that of previously identified molecules.

Defects in coronary vasculogenesis in *Tgfbr3* nulls do not appear to result from defects in angioblast or endothelial differentiation because PECAM-positive cells do appear. A failure in coronary vasculogenesis could result from an insufficient population of angioblasts or endothelial cells, a possibility we cannot exclude because the numbers of these cells was not quantitated. At E14.5, we saw fewer vessels on the heart and a complete absence of large vessels formed by remodeling of the primary vascular plexus. This observation suggests a defect in angioblast or endothelial cell assembly or remodeling. TGFβR3 contains a cytoplasmic PDZ domain that has been shown to bind glycoinositolphosphorylceramide or synectin.[52] In both zebrafish and mouse, deletion of synectin results in specific defects in arterial assembly and patterning,[53] suggesting a possible pathway by which TGFβR3, acting through synectin, may regulate endothelial cell behavior. This is supported by the observation that mice deficient in *Plxnd1*, which also binds synectin,[54] have excessive numbers of small, blood-filled vascular structures on the surface of the heart.[55] The presence of patent coronary ostia in *Tgfbr3* nulls suggests that divergent mechanisms control coronary vasculogenesis and ostia formation. Therefore, despite the greatly reduced size of the coronary vascular network, nascent vessels identify the correct location for ostia formation and presumably initiate the localized apoptosis required for ostia formation.[56]

The ability of TGFβ to recruit vascular smooth muscle is intact in the absence of *Tgfbr3* in coronary and noncoronary vascular beds. In coculture experiments, TGFβ has been implicated in the recruitment of smooth muscle cells by endothelial cells.[35,57] In vitro studies demonstrate that TGFβ induces loss of epithelial character in both proepicardial[58] and epicardial cells[59] and smooth muscle differentiation in epicardial cells.[59] The loss of epithelial character and expression of smooth muscle marker proteins requires ALK5 kinase activity, implicating the canonical TGFβ signaling pathway. However, Smad activation is not sufficient to induce the effects of TGFβ. Vascular smooth muscle differentiation and recruitment appears to occur normally in *Tgfbr3* nulls demonstrating that *Tgfbr3* is not required for these events in vivo. The requirement of coronary vessels for this receptor, whereas other vascular beds appear to form normally in the absence of TGFβR3 suggests that TGFβR3 may be a novel therapeutic target to direct coronary vessel repair or remodeling.

Acknowledgments

We thank Drs Bin Zhou and Scott Baldwin for critically reading the manuscript and members of the laboratories of J.V.B. and C.B.B. for assistance and discussions. We also thank the Vanderbilt Ingram Cancer Center Embryonic Stem Cell Core.

Sources of Funding

This work was supported by NIH grants HL67105 (to J.V.B.), AHA0655129 (to J.V.B.), and GM07347 (to L.A.C.).

Disclosures

None.

References

1. American Heart Association. Heart disease and stroke statistics—2004 update. Dallas, Tex: American Heart Association; 2003.
2. Tomanek RJ. Formation of the coronary vasculature during development. *Angiogenesis*. 2005;8:273–284.
3. Olivey HE, Compton LA, Barnett JV. Coronary vessel development: the epicardium delivers. *Trends Cardiovasc Med*. 2004;14:247–251.
4. Azhar M, Schultz Jel J, Grupp I, Dorn GW 2nd, Meneton P, Molin DG, Gittenberger-de Groot AC, Doetschman T. Transforming growth factor beta in cardiovascular development and function. *Cytokine Growth Factor Rev*. 2003;14:391–407.
5. Muraoka-Cook RS, Dumont N, Arteaga CL. Dual role of transforming growth factor beta in mammary tumorigenesis and metastatic progression. *Clin Cancer Res.* 2005;11:937s–943s.
6. Roberts AB, Wakefield LM. The two faces of transforming growth factor beta in carcinogenesis. *Proc Natl Acad Sci U S A*. 2003;100:8621–8623.
7. Roberts AB, Sporn MB. The transforming growth factor-betas. In: Sporn MB, Roberts AB, eds. *Peptide Growth Factors and Their Receptors.* New York: Springer-Verlag; 1990.
8. Sanford LP, Ormsby I, Gittenberger-de Groot AC, Sariola H, Friedman R, Boivin GP, Cardell EL, Doetschman T. TGFbeta2 knockout mice have multiple developmental defects that are non-overlapping with other TGFbeta knockout phenotypes. *Development*. 1997;124:2659–2670.
9. Hu PP, Datto MB, Wang XF. Molecular mechanisms of transforming growth factor-beta signaling. *Endocr Rev*. 1998;19:349–363.
10. Lin HY, Wang XF, Ng-Eaton E, Weinberg RA, Lodish HF. Expression cloning of the TGF-beta type II receptor, a functional transmembrane serine/threonine kinase. *Cell*. 1992;68:775–785.
11. Ebner R, Chen RH, Shum L, Lawler S, Zioncheck TF, Lee A, Lopez AR, Derynck R. Cloning of a type I TGF-beta receptor and its effect on TGF-beta binding to the type II receptor. *Science*. 1993;260:1344–1348.
12. Bassing CH, Yingling JM, Howe DJ, Wang T, He WW, Gustafson ML, Shah P, Donahoe PK, Wang XF. A transforming growth factor beta type I receptor that signals to activate gene expression. *Science*. 1994;263: 87–89.
13. Lin HY, Moustakas A. TGF-beta receptors: structure and function. *Cell Mol Biol*. 1994;40:337–349.
14. Wrana JL, Attisano L, Wieser R, Ventura F, Massague J. Mechanism of activation of the TGF-beta receptor. *Nature*. 1994;370:341–347.
15. Kretzschmar M, Massague J. SMADs: mediators and regulators of TGF-beta signaling. *Curr Opin Genet Dev*. 1998;8:103–111.
16. Lopez-Casillas F, Cheifetz S, Doody J, Andres JL, Lane WS, Massague J. Structure and expression of the membrane proteoglycan betaglycan, a component of the TGF-beta receptor system. *Cell*. 1991;67:785–795.
17. Wang XF, Lin HY, Ng-Eaton E, Downward J, Lodish HF, Weinberg RA. Expression cloning and characterization of the TGF-beta type III receptor. *Cell*. 1991;67:797–805.
18. Cheifetz S, Bellon T, Cales C, Vera S, Bernabeu C, Massague J, Letarte M. Endoglin is a component of the transforming growth factor-beta receptor system in human endothelial cells. *J Biol Chem*. 1992;267: 19027–19030.
19. Pepper MS. Transforming growth factor-beta: vasculogenesis, angiogenesis, and vessel wall integrity. *Cytokine Growth Factor Rev*. 1997;8: 21–43.
20. Lebrin F, Deckers M, Bertolino P, Ten Dijke P. TGF-beta receptor function in the endothelium. *Cardiovasc Res*. 2005;65:599–608.
21. Oshima M, Oshima H, Taketo MM. TGF-beta receptor type II deficiency results in defects of yolk sac hematopoiesis and vasculogenesis. *Dev Biol*. 1996;179:297–302.
22. Shull MM, Ormsby I, Kier AB, Pawlowski S, Diebold RJ, Yin M, Allen R, Sidman C, Proetzel G, Calvin D, Annunziata N, Doetschman T. Targeted disruption of the mouse transforming growth factor-beta 1 gene results in multifocal inflammatory disease. *Nature*. 1992;359:693–699.
23. Larsson J, Goumans MJ, Sjostrand LJ, van Rooijen MA, Ward D, Leveen P, Xu X, ten Dijke P, Mummery CL, Karlsson S. Abnormal angiogenesis but intact hematopoietic potential in TGF-beta type I receptor-deficient mice. *EMBO J*. 2001;20:1663–1673.
24. Oh SP, Seki T, Goss KA, Imamura T, Yi Y, Donahoe PK, Li L, Miyazono K, ten Dijke P, Kim S, Li E. Activin receptor-like kinase 1 modulates transforming growth factor-beta 1 signaling in the regulation of angiogenesis. *Proc Natl Acad Sci U S A*. 2000;97:2626–2631.
25. Li DY, Sorensen LK, Brooke BS, Urness LD, Davis EC, Taylor DG, Boak BB, Wendel DP. Defective angiogenesis in mice lacking endoglin. *Science*. 1999;284:1534–1537.
26. Chang H, Huylebroeck D, Verschueren K, Guo Q, Matzuk MM, Zwijsen A. Smad5 knockout mice die at mid-gestation due to multiple embryonic and extraembryonic defects. *Development*. 1999;126:1631–1642.
27. Yang X, Castilla LH, Xu X, Li C, Gotay J, Weinstein M, Liu PP, Deng CX. Angiogenesis defects and mesenchymal apoptosis in mice lacking SMAD5. *Development*. 1999;126:1571–1580.
28. Goumans MJ, Valdimarsdottir G, Itoh S, Rosendahl A, Sideras P, ten Dijke P. Balancing the activation state of the endothelium via two distinct TGF-beta type I receptors. *EMBO J*. 2002;21:1743–1753.
29. Goumans MJ, Valdimarsdottir G, Itoh S, Lebrin F, Larsson J, Mummery C, Karlsson S, ten Dijke P. Activin receptor-like kinase (ALK)1 is an antagonistic mediator of lateral TGFbeta/ALK5 signaling. *Mol Cell*. 2003;12:817–828.
30. Lebrin F, Goumans MJ, Jonker L, Carvalho RL, Valdimarsdottir G, Thorikay M, Mummery C, Arthur HM, ten Dijke P. Endoglin promotes endothelial cell proliferation and TGF-beta/ALK1 signal transduction. *EMBO J*. 2004;23:4018–4028.
31. Arthur HM, Ure J, Smith AJ, Renforth G, Wilson DI, Torsney E, Charlton R, Parums DV, Jowett T, Marchuk DA, Burn J, Diamond AG. Endoglin, an ancillary TGFbeta receptor, is required for extraembryonic angiogenesis and plays a key role in heart development. *Dev Biol*. 2000;217: 42–53.
32. Bourdeau A, Dumont DJ, Letarte M. A murine model of hereditary hemorrhagic telangiectasia. *J Clin Invest*. 1999;104:1343–1351.
33. Bartram U, Molin DG, Wisse LJ, Mohamad A, Sanford LP, Doetschman T, Speer CP, Poelmann RE, Gittenberger-de Groot AC. Double-outlet right ventricle and overriding tricuspid valve reflect disturbances of looping, myocardialization, endocardial cushion differentiation, and apoptosis in TGF-beta(2)-knockout mice. *Circulation*. 2001;103:2745–2752.
34. Stenvers KL, Tursky ML, Harder KW, Kountouri N, Amatayakul-Chantler S, Grail D, Small C, Weinberg RA, Sizeland AM, Zhu HJ. Heart and liver defects and reduced transforming growth factor beta2 sensitivity in transforming growth factor beta type III receptor-deficient embryos. *Mol Cell Biol*. 2003;23:4371–4385.
35. Hirschi KK, Rohovsky SA, D'Amore PA. PDGF, TGF-beta, and heterotypic cell-cell interactions mediate endothelial cell-induced recruitment of 10T1/2 cells and their differentiation to a smooth muscle fate. *J Cell Biol*. 1998;141:805–814.
36. Zhang JC, Kim S, Helmke BP, Yu WW, Du KL, Lu MM, Strobeck M, Yu Q, Parmacek MS. Analysis of SM22alpha-deficient mice reveals unanticipated insights into smooth muscle cell differentiation and function. *Mol Cell Biol*. 2001;21:1336–1344.
37. Mikawa T, Fischman DA. Retroviral analysis of cardiac morphogenesis: discontinuous formation of coronary vessels. *Proc Natl Acad Sci U S A*. 1992;89:9504–9508.
38. Mikawa T, Gourdie RG. Pericardial mesoderm generates a population of coronary smooth muscle cells migrating into the heart along with ingrowth of the epicardial organ. *Dev Biol*. 1996;174:221–232.
39. Chen TH-P, Chang T-C, Kang J-O, Choudhary B, Makita T, Tran CM, Burch JBE, Eid H, Sucov HM. Epicardial induction of fetal cardiomyocyte proliferation via a retinoic acid-inducible trophic factor. *Dev Biol*. 2002;250:198–207.
40. Kwee L, Baldwin HS, Shen HM, Stewart CL, Buck C, Buck CA, Labow MA. Defective development of the embryonic and extraembryonic circulatory systems in vascular cell adhesion molecule (VCAM-1) deficient mice. *Development*. 1995;121:489–503.
41. Kang JO, Sucov HM. Convergent proliferative response and divergent morphogenic pathways induced by epicardial and endocardial signaling in fetal heart development. *Mech Dev*. 2005;122:57–65.
42. Tevosian SG, Deconinck AE, Tanaka M, Schinke M, Litovsky SH, Izumo S, Fujiwara Y, Orkin SH. FOG-2, a cofactor for GATA transcription factors, is essential for heart morphogenesis and development of coronary vessels from epicardium. *Cell*. 2000;101:729–739.
43. Yang JT, Rayburn H, Hynes RO. Cell adhesion events mediated by alpha 4 integrins are essential in placental and cardiac development. *Development*. 1995;121:549–560.
44. Sengbusch JK, He W, Pinco KA, Yang JT. Dual functions of $\alpha 4\beta 1$ integrin in epicardial development: initial migration and long-term attachment. *J Cell Biol*. 2002;157:873–882.
45. Kirschner KM, Wagner N, Wagner KD, Wellmann S, Scholz H. The Wilms tumor suppressor Wt1 promotes cell adhesion through transcriptional activation of the {alpha}4integrin gene. *J Biol Chem*. 2006;281: 31930–31939.
46. Moore AW, McInnes L, Kreidberg J, Hastie ND, Schedl A. YAC complementation shows a requirement for Wt1 in the development of epi-

cardium, adrenal gland and throughout nephrogenesis. *Development*. 1999;126:1845–1857.
47. Crispino JD, Lodish MB, Thurberg BL, Litovsky SH, Collins T, Molkentin JD, Orkin SH. Proper coronary vascular development and heart morphogenesis depend on interaction of GATA-4 with FOG cofactors. *Genes Dev*. 2001;15:839–844.
48. Li WE, Waldo K, Linask KL, Chen T, Wessels A, Parmacek MS, Kirby ML, Lo CW. An essential role for connexin43 gap junctions in mouse coronary artery development. *Development*. 2002;129:2031–2042.
49. Smart N, Risebro CA, Melville AA, Moses K, Schwartz RJ, Chien KR, Riley PR. Thymosin beta4 induces adult epicardial progenitor mobilization and neovascularization. *Nature*. 2007;445:177–182.
50. Ward NL, Van Slyke P, Sturk C, Cruz M, Dumont DJ. Angiopoietin 1 expression levels in the myocardium direct coronary vessel development. *Dev Dyn*. 2004;229:500–509.
51. Lavine KJ, Yu K, White AC, Zhang X, Smith C, Partanen J, Ornitz DM. Endocardial and epicardial derived FGF signals regulate myocardial proliferation and differentiation in vivo. *Dev Cell*. 2005;8:85–95.
52. Blobe GC, Liu X, Fang SJ, How T, Lodish HF. A novel mechanism for regulating transforming growth factor beta (TGF-beta) signaling. Functional modulation of type III TGF-beta receptor expression through interaction with the PDZ domain protein, GIPC. *J Biol Chem*. 2001;276: 39608–39617.
53. Chittenden TW, Claes F, Lanahan AA, Autiero M, Palac RT, Tkachenko EV, Elfenbein A, Ruiz de Almodovar C, Dedkov E, Tomanek R, Li W, Westmore M, Singh JP, Horowitz A, Mulligan-Kehoe MJ, Moodie KL, Zhuang ZW, Carmeliet P, Simons M. Selective regulation of arterial branching morphogenesis by synectin. *Dev Cell*. 2006;10:783–795.
54. Linhares Y. Plexin D1 signals to guide endothelial cells. 2005 Meeting of Medical Fellows, May 9–11, 2005. Chevy Chase, Md: Howard Hughes Medical Institute; Abstract.
55. Eralp I, Lie-Venema H, DeRuiter MC, van den Akker NM, Bogers AJ, Mentink MM, Poelmann RE, Gittenberger-de Groot AC. Coronary artery and orifice development is associated with proper timing of epicardial outgrowth and correlated fas ligand associated apoptosis patterns. *Circ Res*. 2005;96:526–534.
56. Velkey JM, Bernanke DH. Apoptosis during coronary artery orifice development in the chick embryo. *Anat Rec*. 2001;262:310–317.
57. Antonelli-Orlidge A, Saunders KB, Smith SR, D'Amore PA. An activated form of transforming growth factor beta is produced by cocultures of endothelial cells and pericytes. *Proc Natl Acad Sci U S A*. 1989;86:4544–4548.
58. Olivey H, Mundell NA, Austin AF, Barnett JV. Transforming growth factor beta stimulates epithelial-mesenchymal transformation in the proepicardium. *Dev Dyn.* 2006;235:50–59.
59. Compton LA, Potash DA, Mundell NA, Barnett JV. Transforming growth factor-beta induces loss of epithelial character and smooth muscle cell differentiation in epicardial cells. *Dev Dyn*. 2006;235:82–93.

Circulation Research
JOURNAL OF THE AMERICAN HEART ASSOCIATION

Coronary Vessel Development Is Dependent on the Type III Transforming Growth Factor β Receptor

Leigh A. Compton, Dru A. Potash, Christopher B. Brown and Joey V. Barnett

Circ Res. published online August 17, 2007;
Circulation Research is published by the American Heart Association, 7272 Greenville Avenue, Dallas, TX 75231

Print ISSN: 0009-7330. Online ISSN: 1524-4571

Supplementary Materials

Generation of null mice

A targeting vector was made to delete exon 3 that encodes the N-terminus, including a portion of the extracellular ligand binding domain. The genomic structure of *Tgfbr3* was determined by searching the Celera database® using the published mouse cDNA. Sequence fragments were assembled using DNASTAR software to generate a single, contiguous genomic sequence that spanned all 17 *Tgfbr3* exons. Oligonucleotides were designed to PCR amplify 5' and 3' arms of homology and *Tgfbr3* exon 3 from 129 SvEvTac mouse genomic DNA. Primers were as follows:Long Arm: Forward 5' GTCGACTTATAAAAGTTTCTGTGAGGA3', Reverse 5' GTCGACGTCAAGGAAACCTCCCAATGG; Short Arm: Forward 5'CTCGAGTAGTTCCTTATTGAGTTACCA3', Reverse 5'CTCGAGACCCTACCTCCTTCTTTCCTATCT3'; exon3: forward 5' GGATCCACACATAAACCTAAAGAGAAATCA3', Reverse 5'CTCGAGTATTGAAGCATATTACATACGATATGCTTCAATATCCAGGAGCAA TGTGTTCT3'. Amplification products were subcloned into pLOX-TKneo after removal of the HSV-TK cassette. The construct was linearized by digestion with NotI (Fig. S1A). ES cells from 129/SvEvTac blastocysts were electroporated with the linearized targeting construct. Seven-hundred G418 resistant clones were screened by Southern blot. One positive clone was expanded and injected into C57BL/6 blastocysts implanted into pseudopregnant female mice. Chimeric mice were mated to C57BL/6 mice and germ line transmission of the targeted allele was confirmed by PCR analysis. 3loxP *Tgfbr3* heterozygotes were mated to EIIa-Cre transgenic mice. Progeny were screened by PCR for null alleles produced by Cre mediated recombination (Fig. S1C). Heterozygous null mice were mated to generate homozygous null mice.

Southern blot and hybridization

Three ^{32}P-labeled DNA probes were used to identify ES cells that underwent homologous recombination. Probe templates external to the 5' and 3' regions of recombination were generated by PCR and an internal probe was generated by releasing the neomycin cassette from pLOX-TKneo with SpeI and BamHI (Fig. 1A). (5' probe template forward 5'TCGAGTAGATATGAAAACACCTT3', reverse 5'TCGAGTAGATATGAAAACACCTT3'; 3' probe template forward 5' TTACAGAAATACTGCATA3', reverse 5' GCCAGGCATGCTCAGACG3'). Genomic DNA from 700 expanded ES cell clones was restriction digested with BglII and SpeI and probed by standard methods (Fig S1B).

Generation of MEFs

E13.5 embryos were harvested in sterile phosphate buffered saline (PBS), minced, and incubated in trypsin EDTA for 30 minutes. The trypsin solution was transferred to culture dishes containing DMEM, 10% FBS, and 1:100 Pen/Strep. This process was repeated until there was no remaining tissue.

RT-PCR

Total RNA was harvested from mouse embryonic fibroblasts (MEFs) (Trizol Reagent-Invitrogen) and further purified with RNeasy Mini Kit (Qiagen). RNA was reverse-transcribed and the resultant DNA was PCR amplified using Titan One Tube RT-PCR kit (Roche). Oligonucleotides were positioned in exons 2 and 5 to determine the presence or absence of exon 3 across genotypes. (forward 5'GCTACACCCGACTTGCCACACT3'; reverse 5'GACCACAGAACCCTCCGAAACC3'). Products were electrophoresed on a 1% agarose/TAE gel (Fig. S1D).

Affinity Labeling with ^{125}I TGFβ

MEFs were cultured to confluence in six well dishes in duplicate. Crosslinking performed as described previously [1] (Fig. S1E).

Histology and Wholemount immunohistochemistry

Embryonic tissue used for hemotoxylin and eosin (H&E) staining was processed by standard methods. For wholemounts, tissue was fixed in 4:1 methanol:DMSO overnight at 4ºC and stained by standard methods [2] (primary antibody to platelet endothelial cells adhesion molecule (PECAM) was at 1:100 (BD).

β-galactosidase staining of transgenic reporter mice

Tgfbr3 +/- mice were crossed to mice harboring the SM22alpha *lacZ* trangene [3] to produce double heterozygotes. Embryos generated by mating double heterozygotes were harvested in PBS, fixed in 2% PFA for two hours, and stained by standard methods [3]. Embryos were washed in PBS and photographed.

Figure S1. Targeting of *Tgfbr3*. A-E. Strategy to generate and confirm *Tgfbr3* targeting. A. *loxP* sites flanking exon 3 and the neomycin resistance cassette were introduced into the *Tgfbr3* locus by homologous recombination. Exon 3 and the neomycin cassette were removed from the targeted allele by Cre-mediated recombination in mice to generate a null allele. B. Southern blot of ES cell DNA digested with BglII and SpeI. Positions of 5', neo and 3' probes are indicated by the patterned bars (A). 5' and 3' probes bind an 8.5 kb and 4.3 kb targeted allele, respectively and an 11 kb wild-type allele. An internal neo probe binds a 4.3 kb fragment. C. PCR amplification of genomic DNA from wt (+/+), heterozygous null (+/-) and null (-/-) mice using oligonucleotides depicted as arrowheads (A). D. RT-PCR using total RNA from +/+, +/- and -/- mouse embryonic fibroblasts (MEFs) demonstrating the absence of the 184 bp exon 3 in the *Tgfbr3* transcript. Forward and reverse oligonucleotides were positioned in exons 2 and 5, respectively, as depicted in the partial map of the cDNA. E. Ligand crosslinking with ^{125}I-TGFβ to MEFs confirms loss of protein expression in nulls.

Figure S2. Smooth muscle recruitment to the coronary ostia occurs in null embryos. A-B. *LacZ*-positive cells are present in the epicardial layer and subepicardium in all genotypes. A. *lacZ*-positive cells are prominently associated with dysmorphic vascular structures in nulls. B. *lacZ*-positive cells are found in association with blood islands in the subepicardium at the apex of the heart (arrowheads). C. At E15.0 *lacZ*-positive cells are associated with large vessels in wild-type hearts.

Table S1. Genotypes of harvested embryos

Stage (E)	+/+	+/-	-/-	total
9.5	1	3	1	5
11.5	8	18	5	31
12.5	6	8	5	19
13.5	25 (1)	53	30 (1)	111
14.5	43 (2)	68	29 (13)	154
15.5	14	16	0 (10)	40
17.5	2	4	0 (4)	10

Number in parentheses indicates embryos dead at harvest

References

1. Brown CB, Boyer AS, Runyan RB, Barnett JV. Requirement of type III TGF-beta receptor for endocardial cell transformation in the heart. *Science.* 1999;283:2080-2082.
2. Brown CB, Drake CJ, Barnett JV. Antibodies directed against the chicken type II TGFbeta receptor identify endothelial cells in the developing chicken and quail. *Dev Dyn.* 1999;215:79-85.
3. Zhang JC, Kim S, Helmke BP, Yu WW, Du KL, Lu MM, Strobeck M, Yu Q, Parmacek MS. Analysis of SM22alpha-deficient mice reveals unanticipated insights into smooth muscle cell differentiation and function. *Mol Cell Biol.* 2001;21:1336-1344.

Figure S1

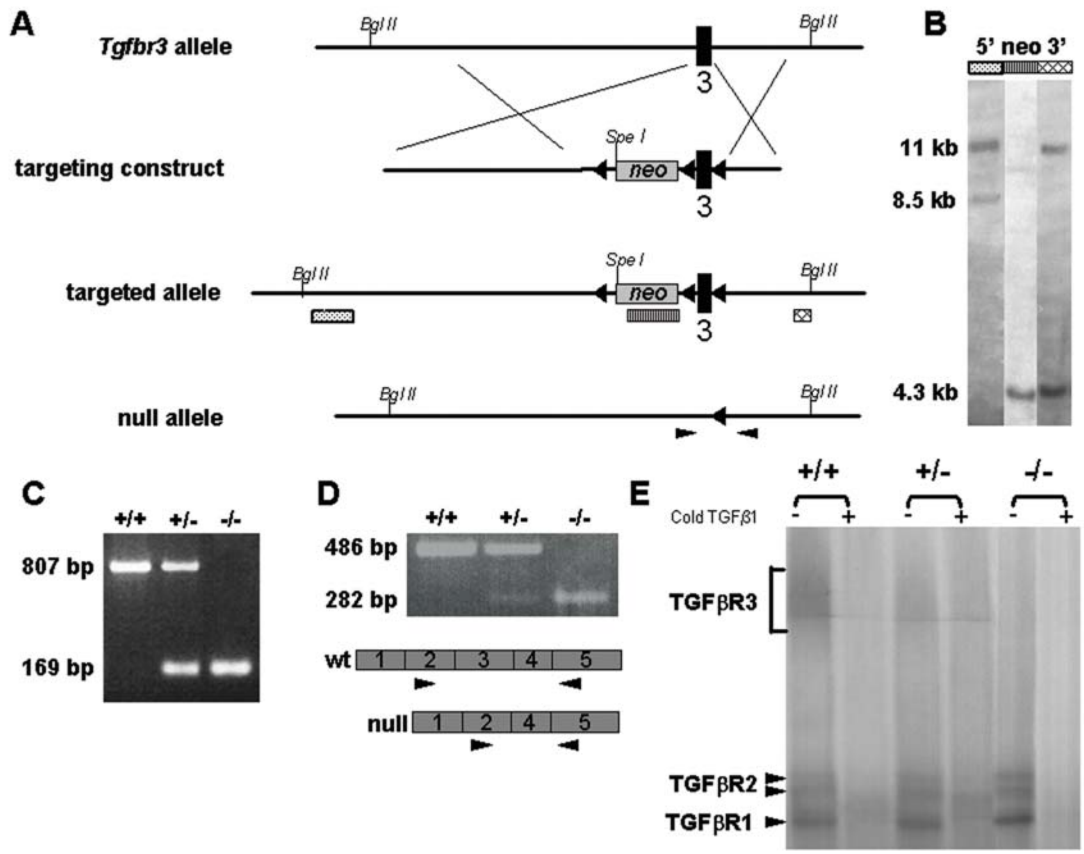
A
Tgfbr3 allele
Bgl II
Bgl II
3
targeting construct
Spe I
neo
3
targeted allele
Bgl II
Spe I
neo
Bgl II
3
null allele
Bgl II
Bgl II
B
5' neo 3'
11 kb
8.5 kb
4.3 kb
C
+/+ +/- -/-
807 bp
169 bp
D
+/+ +/- -/-
486 bp
282 bp
wt 1 2 3 4 5
null 1 2 4 5
E
+/+ +/- -/-
Cold TGFβ1 - + - + - +
TGFβR3
TGFβR2
TGFβR1

Figure S2